Journal of Alloys and Compounds 509 (2011) 5969–5973

Contents lists available at ScienceDirect

Journal of Alloys and Compounds

journal homepage: www.elsevier.com/locate/jallcom

Large-scale synthesis of macroporous SnO_2 with/without carbon and their application as anode materials for lithium-ion batteries

Fei Wang, Gang Yao, Minwei Xu, Mingshu Zhao*, Zhanbo Sun, Xiaoping Song**

MOE Key Laboratory for Non-equilibrium Synthesis and Modulation of Condensed Matter, School of Science, Xi'an Jiaotong University, Shaan Xi 710049, People's Republic of China

ARTICLE INFO

Article history:
Received 10 December 2010
Received in revised form 23 February 2011
Accepted 6 March 2011
Available online 11 March 2011

Keywords:
Tin dioxide
Macroporous
Electrochemical property
Anode
Lithium ion battery

ABSTRACT

The macroporous SnO_2 is prepared using close packed carbonaceous sphere template which synthesized from glucose by hydrothermal method. The structure and morphology of the macroporous SnO_2 are evaluated by XRD and FE-SEM. The average pore size of the macroporous SnO_2 is about 190 nm and its wall thickness is less than 10 nm. When the macroporous SnO_2 filled with carbon is used as an anode material for lithium-ion battery, the capacity is about 380 mAh g^{-1} after 70 cycles. The improved cyclability is attributed to the carbon matrix which is used as an effective physical buffer to prevent the collapse of the well dispersed macroporous SnO_2.

1. Introduction

Lithium-ion batteries are dominating the present portable electronic markets and becoming a good choice for upcoming electric and hybrid vehicles. To meet the demands for high-energy application fields, considerable research efforts have been prompted to develop new electrode materials with higher lithium storage capacity [1–6].

Among a large number of alternative negative materials, SnO_2 has attracted particular interest owing to their high theoretical specific capacity (~790 mAh g^{-1}), widespread availability, low toxicity and low cost. However, the SnO_2 anode suffers the large volume change (>200%) during the lithiation/delithiation processes. This leads to the cracking and crumbling of the electrode materials and results in poor cyclability [7–12]. To enhance the cyclability of SnO_2 anode, several strategies have been proposed. Among them, synthesis of nano-SnO_2 with loose structures, such as nanosheets [13], nanotubes [14], core/shell structures [15], nanowires [16–18], hollow/mesoporous spheres [19–23], and 3D nanostructure [24,25], is a fashionable and effective route. The free spaces in them are significant to accommodate the strain caused by severe volume change. However, most of these loose SnO_2 structures are metastable and could not effectively improve their long-term cyclability. Comparatively, nanocomposite based on active/inactive concept [26] should be more effective to improve the cycling performance of SnO_2. Carbon materials are usually used as the inactive buffer material due to its soft nature and good electronic conductivity [27–34]. For example, porous SnO_2 nanotubes with coaxially grown carbon nanotube overlayers [27] and nanostructured Sn–C composite with Sn nanoparticles finely dispersed in a supporting carbon matrix [34] exhibit superior cyclability over 200 cycles. Understandably, if the free spaces of loose SnO_2 nanostructures are densely filled with carbon, the cyclability would be obviously improved due to the combination of nanostructure design and the active/inactive nanocomposite concept [28,31].

Here we report a new and facile template method to synthesize macroporous SnO_2 in large-scale. The carbonaceous spheres made from glucose are used as hard template instead of other conventional organic (such as polystyrene [35,36]) and silica [37,38] templates. This method is based on the precipitation of Sn salt precursors in the close packed carbonaceous sphere template and subsequent chemical conversion of the precursors to tin dioxide. The carbonaceous sphere template in macroporous SnO_2 can be removed or maintained selectively by changing the calcination condition. The electrochemical properties of macroporous SnO_2 with/without carbon matrix have also been investigated.

2. Experimental

2.1. Synthesis of carbonaceous sphere template

A solution was made by dissolving 2.4771 g glucose in 25 ml deionized water through ultrasonic dispersion. Afterward, the clear solution was transferred to

* Corresponding author. Tel.: +86 29 82663034; fax: +86 29 82667872.
** Corresponding author. Tel.: +86 29 82665892; fax: +86 29 82667872.
E-mail addresses: zhaomshu@mail.xjtu.edu.cn (M. Zhao), xpsong@mail.xjtu.edu.cn (X. Song).

0925-8388/$ – see front matter © 2011 Elsevier B.V. All rights reserved.
doi:10.1016/j.jallcom.2011.03.041

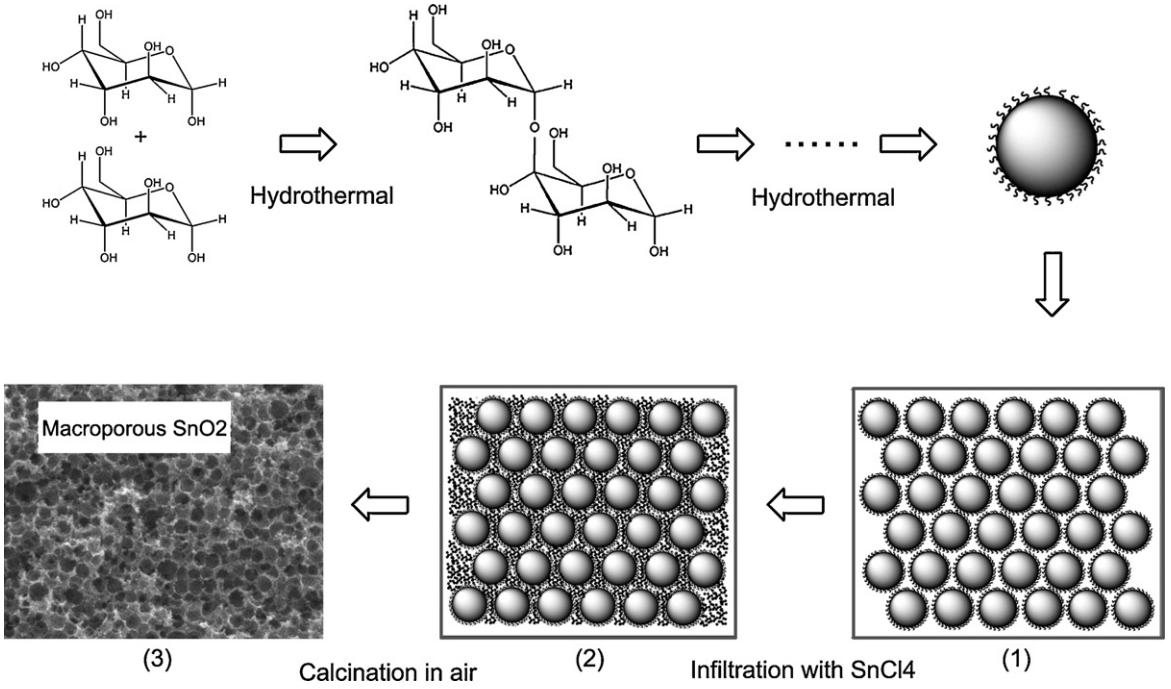

Fig. 1. Schematic illustration for the synthetic procedure of macroporous SnO_2.

Teflon lined stainless steel autoclaves and hydrothermally treated in oven at 180 °C for 4 h. After cooling down naturally, the dark grey solution was obtained.

2.2. Synthesis of macroporous SnO_2 with/without carbon matrix

A solution was made by dissolving 0.3156 g $SnCl_4$ in 80 ml deionized water and then it was mixed with 20 ml as-prepared carbonaceous sphere solution. The mixed solution was treated by ultrasonic vibration for 40 min to ensure sufficient diffusion of the metal ions. The black precipitates were harvested by centrifugation and washed thoroughly with deionized water and alcohol, respectively. The obtained samples were dried in oven at 60 °C for 2 h. The dried samples were loaded in porcelain boat and then heated in furnace at 550 °C for 4 h in air or argon.

2.3. Sample characterization

The structure and morphology of the products were characterized by X-ray powder diffraction (XRD, Bruke D8-Advance, Cu-Kα, λ = 0.15406 nm), X-ray photoelectron spectroscopy (XPS, Kratos Axis Ultra, Al-Kα, $h\nu$ = 1486.6 eV), field emission scanning electron microscope (FESEM, JEOL JSM-7100F) and transmission electron microscopy (TEM, JEOL JEM-2100).

2.4. Electrochemical measurements

Electrochemical properties of the macroporous SnO_2 with/without carbon matrix were tested with two-electrode Swagelok cells. The working electrodes were prepared as the follows. The mixture was made by mixing active material, carbon black, and binder (polyvinylidene fluoride, PVDF) at a mass ratio of 80:10:10. Subsequently, it was dispersed in N-methyl pyrrolidinone (NMP). Then, the slurry was coated uniformly onto a copper foil with a diameter of 10 mm and dried at 110 °C for 12 h in vacuum. Test cells were assembled in argon filled glove box. Metallic lithium foil was used as the counter electrode. The electrolyte was 1 M $LiPF_6$ in a mixture of 50 vol.% ethylene carbonate (EC) and 50 vol.% diethylene carbonate (DEC). The galvanostatical charge and discharge measurement was carried out on Arbin BT2000 battery testing system at a current density of 0.2 mA cm^{-2} in the voltage range of 0.02–2.0 V (vs. Li/Li^+). The cyclic voltammograms (CV) were tested on Ametek VMC-4 electrochemical testing system at a scan rate of 0.3 mV s^{-1} between 0 V and 2.0 V (vs. Li/Li^+).

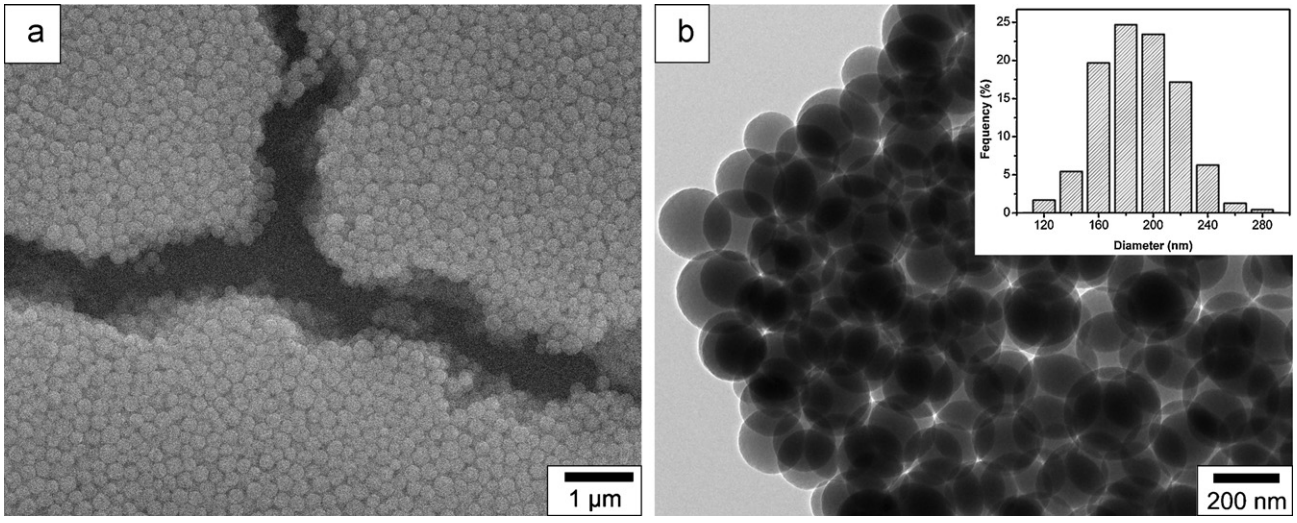

Fig. 2. SEM image (a) and TEM image (b) of carbonaceous spheres. The inset of (b) shows the size distributions of carbonaceous spheres.

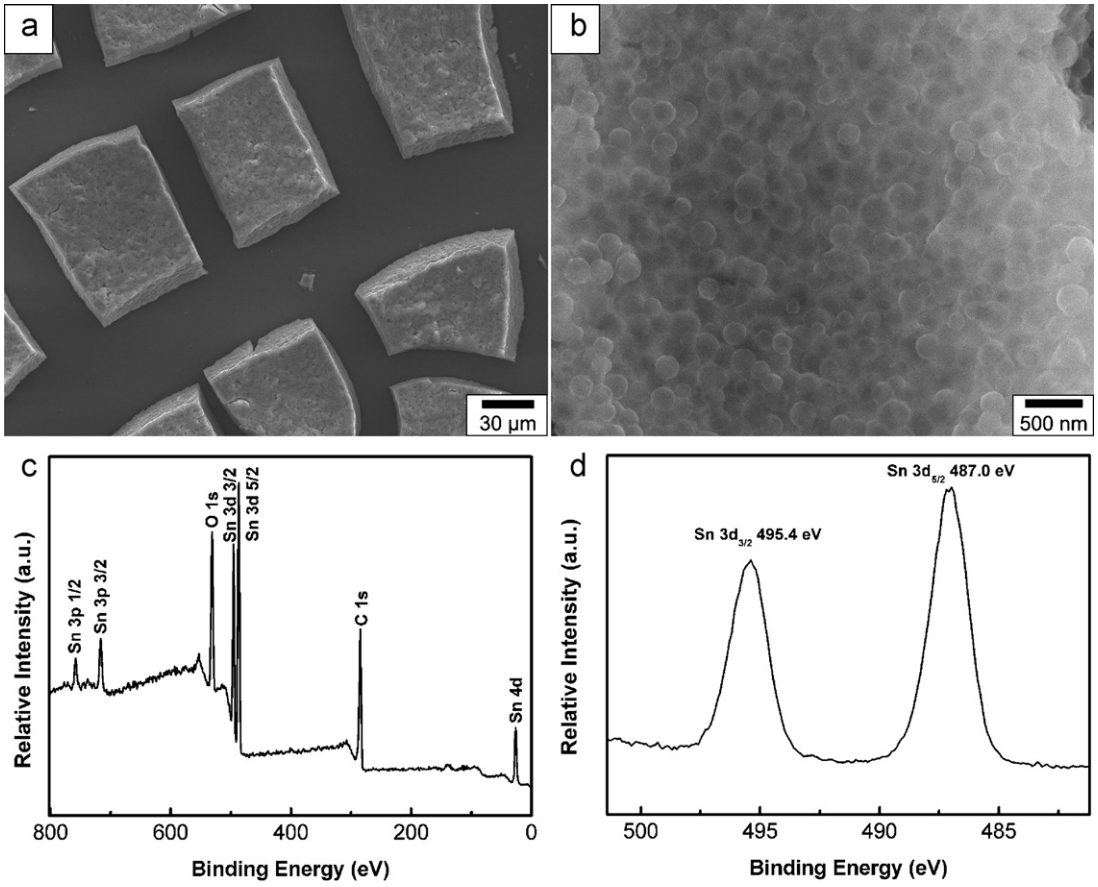

Fig. 3. SEM images (a and b) of carbonaceous sphere/Sn^{4+} composites; survey (c) and Sn 3d (d) XPS spectrums of carbonaceous sphere/Sn^{4+} composites.

3. Results and discussion

The synthetic method of macroporous SnO_2 is schematically illustrated in Fig. 1. Firstly, the carbonaceous spheres with hydrophilic surface were prepared from 0.5 mol L^{-1} glucose aqueous solution under hydrothermal conditions at 180 °C for 4 h. As we know that, chemical reactions of glucose under hydrothermal condition are complex, which make it difficult to determine the exact reaction processes in the sealed vessel. While it is generally accepted that the diameter of the carbonaceous spheres is influenced by the concentration of starting materials, reaction temperature and reaction time [39]. In this experiment, relatively low reactant concentration and short reaction time were used, which lead to the inadequate growth of carbonaceous spheres. Fig. 2a and b displays the SEM and TEM images of the as-prepared carbonaceous spheres. The size distributions are given in the inset of Fig. 2b. It is found that the carbonaceous spheres exhibit narrow size distribution and the average diameter of them is about 190 nm. Furthermore, the carbonaceous spheres tend to aggregate intensively and form close packed products (Fig. 2a).

Then, $SnCl_4$ solution was dispersed into the carbonaceous sphere solution by ultrasonic vibration. As shown in Fig. 3a and b, the obtained composites are agglomeratic blocks with numerous carbonaceous spheres. The surfaces and voids of the close packed carbonaceous spheres are bonded and infiltrated with Sn sources. To further characterize the products, XPS analysis was used to investigate the surface compositions and chemical states of the as-prepared composites. The survey XPS spectrum shown in Fig. 3c indicates that the composites contain Sn, O and C (H cannot be detected by XPS). The high resolution XPS spectrum for Sn 3d was also performed (Fig. 3d). It shows two characteristic peaks of Sn $3d_{5/2}$ and Sn $3d_{3/2}$ at ~487.0 and ~495.4 eV, respectively. Thus, we can conclude that the chemical state of Sn in the as-prepared composites is Sn^{4+}. The existence of Sn^{4+} in the composites is due to the hydrophilic characteristic of carbonaceous sphere surfaces which functionalized with OH and C=O groups. When the metal salt precursors are dispersed in the carbonaceous sphere solution, the functional groups in the surface layer are able to bond metal cations through coordination or electrostatic interactions [40].

Finally, macroporous structure products were obtained by calcining the as-prepared carbonaceous sphere/Sn^{4+} composites at 550 °C for 4 h in air. Fig. 4a shows the overall morphology of the macroporous products. From it we can clearly see that the macroporous products can be obtained in large scale and the size reaches to tens of microns. To further determine the microstructure of the macroporous products, the surface and interior morphology of the products were observed at high magnification by SEM, as shown in Fig. 4b and c. These images clearly reveal that both the surface and interior are macroporous structure. The pore size of macroporous products is similar to the diameter of carbonaceous spheres. The wall of the macroporous structure is composed of monolayer SnO_2 nanoparticles and its thickness is about ~10 nm, which is the particle size of the SnO_2 showed in the inset HRTEM image of Fig. 4c. The inset of Fig. 4a shows the XRD pattern of the macroporous products. All diffraction peaks can be indexed as tetragonal rutile SnO_2 (JCPDS Card No. 41-1445, space group P42/mnm, a_0 = 4.738 Å, c_0 = 3.187 Å). The diffraction peaks are relatively broad. By using the Scherrer's formula and the full width at half maximum (FWHM) data of (1 1 0) peak, the mean crystallite size can be calculated to be equal to 7.3 nm. The calculated crystallite size is consistent with the result obtained by HRTEM. Furthermore, the as-prepared carbonaceous sphere/Sn^{4+} composites were also calcined at 550 °C for 4 h in

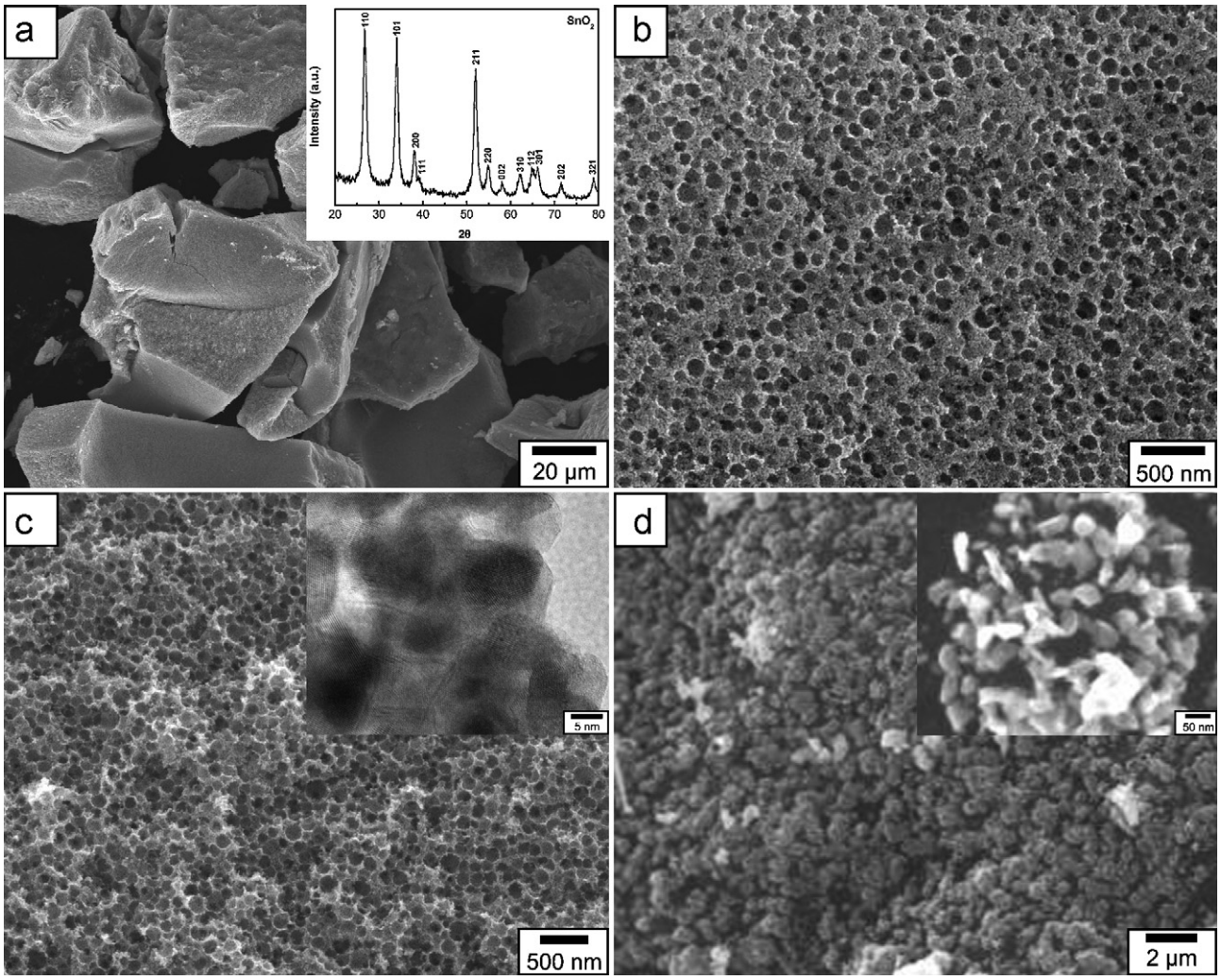

Fig. 4. Survey (a), surface (b), and interior (c) SEM images of macroporous SnO_2; SEM image of SnO_2/C composites (d). The inset of (a) is the XRD pattern of macroporous SnO_2, the inset of (c) is the HRTEM image of macroporous SnO_2 and the inset of (d) is the high magnification SEM image of SnO_2/C composites.

argon. The carbonaceous spheres transform to carbon spheres and compact SnO_2/C composites instead of macroporous SnO_2 were obtained. As shown in Fig. 4d, we can see that the particle size of SnO_2 is larger than macroporous SnO_2, which should be ascribed to the aggregation of SnO_2 on the carbon surface.

As anode materials for lithium-ion batteries, the lithium storage properties of macroporous SnO_2 with/without carbon are evaluated using a two-electrode cell. The charge/discharge reactions of SnO_2 with Li can be described as follows:

$$SnO_2 + 4Li^+ + 4e^- \rightarrow Sn + 2Li_2O; \quad (1)$$

$$Sn + xLi^+ + xe^- \leftrightarrow Li_xSn \quad (0 \leq x \leq 4.4). \quad (2)$$

Fig. 5a shows the cyclic voltammetry (CV) curves for the first five cycles of macroporous SnO_2. In the first cathodic scan, the peak near 0.7 V can be ascribed to the formation of solid electrolyte interface (SEI) films and the reduction of SnO_2. The broad peak at about 0.1 V corresponds to the lithiation reaction of Sn, which can be described as Eq. (2). In the first anodic scan, there are also two obvious peaks. The first peak near 0.6 V stems from the delithiation reaction of Li_xSn and the relatively weaker peak at about 1.2 V should correspond to the reduction of Li_2O. It is generally accepted that the reaction of Eq. (1) is irreversible in SnO_2 electrodes. However, in the macroporous SnO_2 electrode, the peak at high voltage, i.e., the 1.0 V peak in anodic scan and 1.2 V peak in cathodic scans, can reappear in the following cycles. It means that the first reaction process as described in Eq. (1) is partially reversible, which is consistent with previous work [41,42]. The partially reversible reaction of Eq. (1) results in high capacity of macroporous SnO_2.

The cycle performance of macroporous SnO_2 electrode is shown in Fig. 5b. The initial discharge and charge capacities are 2005 and 1019 mAh g^{-1}, respectively. The large irreversible capacity of first cycle is attributed to the decomposition of electrolyte, the formation of solid electrolyte interface (SEI) film on the electrode surfaces and the partially irreversible reaction of Eq. (1). From the cycling performance curves, we can see that the cyclability of macroporous SnO_2 is not satisfactory although it has high capacities in first several cycles. The capacities of macroporous SnO_2 in the 20th cycle can achieve at 631 mAh g^{-1}, while the capacities decrease to 297 mAh g^{-1} in the 50th cycle. The poor cyclability should be attributed to the collapse of the loose SnO_2 nanostructure during the lithiation/delithiation process for the lack of a supporting matrix.

The electrochemical performance of macroporous SnO_2 with carbon matrix was also evaluated to investigate the influence of supporting matrix to loose SnO_2 nanostructure. From Fig. 5b we can clearly see that the cycling performance of SnO_2/C composites was obviously improved and the capacities in the 70th cycle

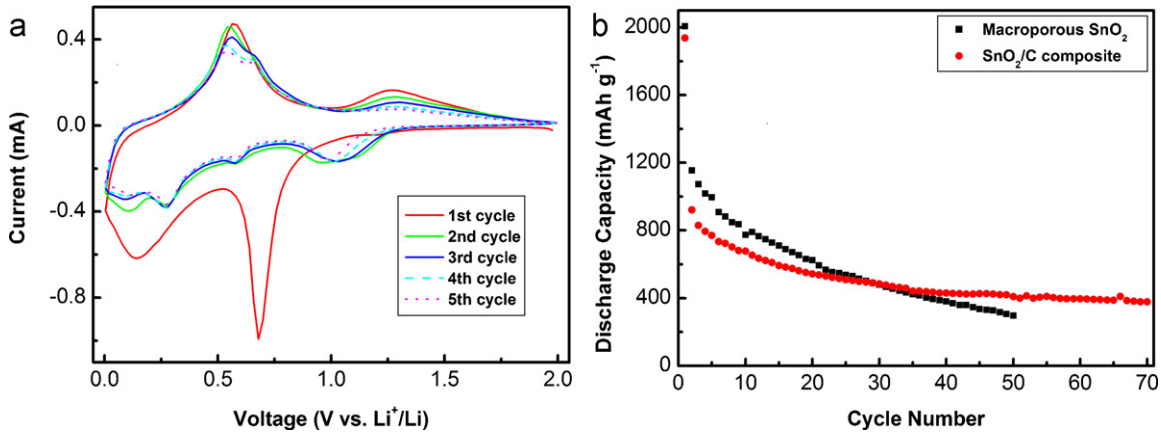

Fig. 5. CV curves of macroporous SnO_2 (a) and cycling performance of macroporous SnO_2 and SnO_2/C composites (b).

maintain at about 380 mAh g^{-1}. Thus, the carbon served as physical buffer can effectively prevent the collapse of the macroporous SnO_2.

4. Conclusion

In conclusion, we demonstrated a facile synthetic method for preparing macroporous SnO_2 in large-scale using carbonaceous sphere template which prepared from the glucose. The pore size of macroporous SnO_2 is about 190 nm and its wall thickness is less than 10 nm. The electrochemical tests showed that macroporous SnO_2 has high capacities but poor cycling performance. However, the cyclability was effectively improved when the pores of macroporous SnO_2 were filled with carbon Therefore, combining the nanostructure design and active/inactive nanocomposite concept should be an effective way to improve the electrochemical performance of SnO_2 anode.

Acknowledgments

This work was supported by National Natural Science Foundation of China (51002117 and 50871081), the National Basic Research Program of China (2010CB635101) and Fundamental Research Funds for the Central Universities (0109-08141012).

References

[1] Y. Idota, T. Kubota, A. Matsufuji, Y. Maekawa, T. Miyasaka, Science 276 (1997) 1395–1397.
[2] P. Poizot, S. Laruelle, S. Grugeon, L. Dupont, J.M. Tarascon, Nature 407 (2000) 496–499.
[3] K.T. Nam, D.W. Kim, P.J. Yoo, C.Y. Chiang, N. Meethong, P.T. Hammond, Y.M. Chiang, A.M. Belcher, Science 312 (2006) 885–888.
[4] L. Taberna, S. Mitra, P. Poizot, P. Simon, J.M. Tarascon, Nat. Mater. 5 (2006) 567–573.
[5] C.K. Chan, H.L. Peng, G. Liu, K. McIlwrath, X.F. Zhang, R.A. Huggins, Y. Cui, Nat. Nanotechnol. 3 (2008) 31–35.
[6] A. Magasinski, P. Dixon, B. Hertzberg, A. Kvit, J. Ayala, G. Yushin, Nat. Mater. 9 (2010) 353–358.
[7] J.M. Tarascon, M. Armand, Nature 414 (2001) 359–367.
[8] I.A. Courtney, J.R. Dahn, J. Electrochem. Soc. 144 (1997) 2045–2052.
[9] M. Winter, J.O. Besenhard, M.E. Spahr, P. Novak, Adv. Mater. 10 (1998) 725–763.
[10] M. Winter, J.O. Besenhard, Electrochim. Acta 45 (1999) 31–50.
[11] I.A. Courtney, J.R. Dahn, J. Electrochem. Soc. 144 (1997) 2943–2948.
[12] N.C. Li, C.R. Martin, J. Electrochem. Soc. 148 (2001) A164–A170.
[13] C. Wang, Y. Zhou, M.Y. Ge, X.B. Xu, Z.L. Zhang, J.Z. Jiang, J. Am. Chem. Soc. 132 (2010) 46–47.
[14] J.F. Ye, H.J. Zhang, R. Yang, X.G. Li, L.M. Qi, Small 6 (2010) 296–306.
[15] D. Deng, J.Y. Lee, Chem. Mater. 20 (2008) 1841–1846.
[16] M.S. Park, Y.M. Kang, G.X. Wang, S.X. Dou, H.K. Liu, Adv. Funct. Mater. 18 (2008) 455–461.
[17] H. Kim, J. Cho, J. Mater. Chem. 18 (2008) 771–775.
[18] M.S. Park, G.X. Wang, Y.M. Kang, D. Wexler, S.X. Dou, H.K. Liu, Angew. Chem. Int. Ed. 46 (2007) 750–753.
[19] Y. Yu, C.H. Chen, Y. Shi, Adv. Mater. 19 (2007) 993–997.
[20] R. Demir-Cakan, Y.S. Hu, M. Antonietti, J. Maier, M.M. Titirici, Chem. Mater. 20 (2008) 1227–1229.
[21] H.X. Yang, J.F. Qian, Z.X. Chen, X.P. Ai, Y.L. Cao, J. Phys. Chem. C 111 (2007) 14067–14071.
[22] Y. Wang, F.B. Su, J.Y. Lee, X.S. Zhao, Chem. Mater. 18 (2006) 1347–1353.
[23] X.W. Lou, Y. Wang, C.L. Yuan, J.Y. Lee, L.A. Archer, Adv. Mater. 18 (2006) 2325–2329.
[24] J.C. Lytle, H.W. Yan, N.S. Ergang, W.H. Smyrl, A. Stein, J. Mater. Chem. 14 (2004) 1616–1622.
[25] Y. Yu, L. Gu, A. Dhanabalan, C.H. Chen, C.L. Wang, Electrochim. Acta 54 (2009) 7227–7230.
[26] A.S. Arico, P. Bruce, B. Scrosati, J.M. Tarascon, W. Van Schalkwijk, Nat. Mater. 4 (2005) 366–377.
[27] Y. Wang, H.C. Zeng, J.Y. Lee, Adv. Mater. 18 (2006) 645–649.
[28] J. Liu, W. Li, A. Manthiram, Chem. Commun. 46 (2010) 1437–1439.
[29] Y.S. Lin, J.G. Duh, D.T. Shieh, M.H. Yang, J. Alloys Compd. 490 (2010) 393–398.
[30] G.D. Du, C. Zhong, P. Zhang, Z.P. Guo, Z.X. Chen, H.K. Liu, Electrochim. Acta 55 (2010) 2582–2586.
[31] X.W. Lou, D. Deng, J.Y. Lee, L.A. Archer, Chem. Mater. 20 (2008) 6562–6566.
[32] Z.H. Wen, Q. Wang, Q. Zhang, J.H. Li, Adv. Funct. Mater. 17 (2007) 2772–2778.
[33] C.Q. Feng, L. Li, Z.P. Guo, H. Li, J. Alloys Compd. 504 (2010) 457–461.
[34] G. Derrien, J. Hassoun, S. Panero, B. Scrosati, Adv. Mater. 19 (2007) 2336–2340.
[35] Z.Y. Zhong, Y.D. Yin, B. Gates, Y.N. Xia, Adv. Mater. 12 (2000) 206–209.
[36] B.T. Holland, C.F. Blanford, A. Stein, Science 281 (1998) 538–540.
[37] P. Jiang, J. Cizeron, J.F. Bertone, V.L. Colvin, J. Am. Chem. Soc. 121 (1999) 7957–7958.
[38] Y.A. Vlasov, N. Yao, D.J. Norris, Adv. Mater. 11 (1999) 165–169.
[39] X.M. Sun, Y.D. Li, Angew. Chem. Int. Ed. 43 (2004) 597–601.
[40] X.M. Sun, J.F. Liu, Y.D. Li, Chem.—Eur. J. 12 (2006) 2039–2047.
[41] M. Mohamedi, S.J. Lee, D. Takahashi, M. Nishizawa, T. Itoh, I. Uchida, Electrochim. Acta 46 (2001) 1161–1168.
[42] S.J. Han, B.C. Jang, T. Kim, S.M. Oh, T. Hyeon, Adv. Funct. Mater. 15 (2005) 1845–1850.